A covalently cross-linked gel derived from the epidermis of the pilot whale *Globicephala melas*

C. Baum [a,b], L.-G. Fleischer [b,*], D. Roessner [c], W. Meyer [d] and D. Siebers [a]

[a] *Alfred Wegener Institute Foundation for Polar and Marine Research, Am Handelshafen 12, D-27570 Bremerhaven, Germany*

[b] *Institute of Food Technology and Center of Biotechnology, Technical University of Berlin, Amrumer Str. 32, D-13353 Berlin, Germany*

[c] *Wyatt Technology Deutschland GmbH, In der Steubach 9, D-57614 Woldert, Germany*

[d] *Anatomical Institute, Department of Histology and Embryology, School of Veterinary Medicine, Bischofsholer Damm 15, D–30173 Hannover, Germany*

Abstract. The rheological properties of the stratum corneum of the pilot whale (*Globicephala melas*) were investigated with emphasis on their significance to the self-cleaning abilities of the skin surface smoothed by a jelly material enriched with various hydrolytic enzymes. The gel formation of the collected fluid was monitored by applying periodic-harmonic oscillating loads using a stress-controlled rheometer. In the mechanical spectrum of the gel, the plateau region of the storage modulus G' (<1200 Pa) and the loss modulus G'' (>120 Pa) were independent of frequency (ω = 43.98 to 0.13 rad·s^{-1}, τ = 15 Pa, T = 20°C), indicating high elastic performance of a covalently cross-linked viscoelastic solid. In addition, multi-angle laser light scattering experiments (MALLS) were performed to analyse the potential time-dependent changes in the weight-average molar mass of the samples. The observed increase showed that the gel formation is based on the assembly of covalently cross-linked aggregates. The viscoelastic properties and the shear resistence of the gel assure that the enzyme-containing jelly material smoothing the skin surface is not removed from the stratum corneum by shear regimes during dolphin jumping. The even skin surface is considered to be most important for the self-cleaning abilities of the dolphin skin against biofouling.

Keywords: Skin, rheology, gel formation, whales, *Globicephala melas*, self-cleaning abilities, multi-angle laser light scattering (MALLS)

1. Introduction

Integuments represent the segregating layers and interphases between multicellular organisms and their environments. They must provide all necessary exchanges of information and matter between the inner-organismic and external spaces. For biofouling organisms, integuments are the substratum of settlement, thus representing specific types of habitats. Skin covered with biofoulers is – as a rule – disadvantageous for the host.

Among marine organisms a variety of defence strategies against biofouling have been evolved and include continuous and discontinuous mechanisms. Such mechanisms, being based on the physical and biochemical equipment, modify the morphology of the affected body surfaces in order to prevent or

* Address for correspondence: Prof. Dr. Lutz-Günther Fleischer, Institute of Food Technology and Center of Biotechnology, Technical University of Berlin, Amrumer Str. 32, D-13353 Berlin, Germany. Fax: ++49 30 314 275 18; E-mail: l-g.fleischer@gmx.de.

reduce the attachment of microalgae and other microorganisms, or use specific biochemicals directed against them [14,36,37]. Physical defences are based, for example, on the discontinuous desquamation of parts of the superficial body surface, the continuous secretion of mucus and social cleaning. Biochemicals, such as toxins and antibiotics, are produced in order to directly counteract biofoulers, whereas enzymes and surface active substances increase the rate of detachment of organisms from integumental surfaces (e.g., [1,2]).

Our interest focusses on the marine dolphins, which visually exhibit remarkably clean and smooth epidermal surfaces [5,8]. Considering the self-cleaning abilities in dolphins, more than one defence strategy against biofouling seems to be involved in combination. It has been reported, that the skin of dolphins is characterized by low critical surface tension [19,20] and high rates of desquamation [13,21,32]. Employing cryo-scanning microscopical techniques [5,6,8], we demonstrated an average nanorough plane surface of the skin of the pilot whale, that was smoothed by gel. We suppose that the presence of a smooth skin surface reduces the number and quality of microniches, i.e., hiding-places for biofouling organisms, and thus facilitates their detachment from the skin surface by the kinetic and desorptive forces of the water flow, or air bubbles formed during dolphin jumping. In addition, various hydrolytic enzymes were demonstrated in the stratum corneum of the pilot whale. These probably digest the adhesive substances produced by biofouling organisms [7]. Since these hydrolytic enzymes were found in an aggregate-attached form, rheological experiments with dolphin skin in parallel to multi-angle laser light scattering (MALLS) measurements were designed in the course of the study in order to establish details on the formation of these aggregates.

We provide new insights in the macromolecular coating of the skin of the pilot whale, and suggest an important role of the observed jelly skin cover in the self-cleaning properties of the delphinid integument.

2. Material and methods

2.1. Sample preparation

The superficial system of the skin, the stratum corneum, was collected from long-finned pilot whales, *Globicephala melas*, during three authorized hunts of Faroese people in 1999 (for details see [11]). The material was manually obtained from approximately 90 individuals (approx. 90 m^2, excess of sample material approx. 5 $g \cdot m^{-2}$) of both genders and of various ages by means of rotating movements of a stainless steel brush. Care was taken to avoid sampling the living cells of the underlying stratum spinosum. If samples could be further processed within four hours, pooled samples of stratum corneum were stored in vacuum containers at 4°C. If not, they were stored in liquid nitrogen at −196°C immediately after collection. The abraded fresh or deep-frozen flaky samples were transferred into Eppendorf cups, where they warmed up to room temperature during centrifugation (Labofuge, Hettich, equipped with a tilt angle rotor) at 3000 U/min or 4000 U/min for 10 minutes. The Eppendorf cups were perforated with a small hole at the bottom and inserted in plastic tubes which collected the liquid skin material separated by centrifugation. The non-liquid part of the flaky stratum corneum did not pass through the hole. Analyses were performed using the supernatant of the centrifuged sample (approximately 0.1 ml sample volume per g of the centrifuged sample). Dilutions of the supernatant were prepared with isotonic sodium chloride solution (0.9% NaCl). Since we found that the centrifuged stratum corneum was highly enriched with glycoproteins [7], we used ovalbumin in the Bradford protein assay (Sigma), and

the signals of the differential refractive index detector (see below) for measuring the protein concentration of the samples. When employing multi-angle laser light scattering, L-cysteine (Sigma) was added to aliquots of the diluted samples to occupy the free thiol groups.

2.2. *Multi-angle laser light scattering*

Working solutions prepared from 10 independent preparations of the centrifuged flaky material were diluted with isotonic NaCl (approx. 1 : 500 v/v, 1.25×10^{-4} g·ml^{-1}), and stirred with a magnetic stirrer at 23°C temperature in a membrane-sealed glass for more than 12 hours. 2 ml aliquots were injected at time intervals of about 45 minutes in a flow of 0.15 ml·min^{-1} isotonic NaCl solution driven by a HPLC pump (Knauer). This was followed by an ultraviolet light detector (280 nm, MiltonRoy), and the DAWN DSP multi-angle laser light scattering detector (633 nm, Wyatt Technology) to determine the weight-average molar mass M_w and the corresponding z-average root mean square (rms) radii of the batch sample after the signal reached plateau level. Finally it was passed through a differential refractive index (DRI) detector (633 nm, Optilab 903, Wyatt Technology) to measure the concentration of the sample. The DAWN was calibrated against toluene. Absolute molar masses were calculated using Zimm–Berry plot $(K \cdot c \cdot R_\vartheta^{-1})^{0.5}$ versus concentration and the scattering angle ϑ, where K is the light scattering constant for vertically polarized incident light, c is the concentration, and R_ϑ is the Rayleigh ratio at the scattering angle ϑ (Astra software, Wyatt Technology). Scattering angles between 38.8° and 110.7° were used for extrapolation to the scattering angle zero. The data of the light scattering signals were correlated with the concentrations measured by refractive index detector (for theoretical details see [7,38]).

2.3. *Transmission electron microscopy*

The originally liquid-centrifuged, abraded stratum corneum samples of the pilot whale formed an elastic biogel when exposed to air for approx. 4 hours at room temperature. Aliquots of this jelly material were fixed in 2% glutaraldehyde in 0.05 mol·l^{-1} (pH 7) PIPES buffer (piperazine-N,N′-bis[2-ethanesulfonic acid]) for 45 minutes, then rinsed in buffer to remove excess fixatives, and postfixed in 2% osmium acid. Samples were then embedded in EPON 815. Ultrathin sections were contrasted with lead citrate, and viewed in the transmission electron microscope CEM 902 (Zeiss) at 80 kV.

2.4. *Rheology*

The application of harmonic-periodic loads in dynamic rheological measurements is especially suited for structural investigations in order to avoid rheodestructive impact on the structures. Considering the centrifuged stratum corneum, oscillatory measurements were performed in this study employing the rheometer RheoStress RS 150 (Haake) alternatively equipped with two geometries, cone-and-plate (dia = 35 mm, apex angle 1°) or a plate-and-plate (dia = 60 mm) under deformation-controlled or stress-controlled conditions. During the measurements, humidity was held constant for 9 hours with a wet paper sheet within a chamber made from a plastic top, covering the tools and the peltier element holder. This ensured that drying effects at the outer edge of the plates could be excluded. The data used for calculations always originated from the first 8 hours of the 24 hour long-term experimental surveys. Gel kinetic experiments were prolonged until G' reached plateau level (after approx. 5 hours). Frequency and deformation sweeps were performed after the gel had formed as indicated by the plateau level of G'.

2.4.1. Parameters and notation

In stress-controlled measurements, an applied harmonic-periodic sinusodial stress $\tau^*(t) = \tau_0^* e^{i\omega t}$ with the angular frequency $\omega = 2\pi\nu$ is followed by a phase-shifted sinusoidal strain $\gamma^*(t) = \gamma_0^* e^{i\omega t}$ with the same frequency due to the deformation induced. Focussing on the changes of energy densities during gel formation, the complex amplitudes of the stress τ_0^* and the strain γ_0^* were used for calculation of the magnitude of the complex modulus $G^*(i\omega)$, the storage modulus G', and the loss modulus G'' [18]. Analyses of the dynamic biophysical sol-gel system were performed from the gel properties, given by $G'(\omega) = |G^*(i\omega)| \cos \delta(\omega)$, and dynamic viscosity $n'(\omega)$.

3. Results

3.1. Multi-angle laser light scattering

Batches of the abraded and centrifuged stratum corneum samples were measured by multi-angle laser light scattering at various time after dilution (Fig. 1(a), (b)). We observed a time-dependent large increase in the molar mass (M_w) of the samples. It is remarkable, that the molar mass increased exponentially at this considerably high dilution (varying about a dilution of 1 : 500 v/v, corresponding to $1.25 \cdot 10^{-4}$ g·ml^{-1}) of the stratum corneum samples. In absence of better estimate the data obtained were fitted by the Marquardt–Levenberg algorithm seeking the parameters that minimize the sum of the squared differences between the values of the observed and predicted values of the dependent variable using second order rational function ($y_0 = 11.7 \cdot 10^6, a = 5.8 \cdot 10^6, b = 8.7 \cdot 10^6$ for $f = y_0 + ax + bx^2$, regression coefficient $r^2 = 0.999$). In addition, good fitting results (error of estimate between 0.0287 to 0.0033) were obtained applying the composite fitting functions (such as, for example, Chapman's sigmoidal function and exponential functions, such as, for example, rectangular hyperbolic function): $f = y_0 + a(1 - \exp(\cdot bx)^c) + dx/(e + x)$.

At the beginning of the experiment (t_0), the molar masses ranged around $10–30 \cdot 10^6$ g · mol^{-1}, whereas after 5.5 hours M_w amounted to about $100–300 \cdot 10^6$ g·mol^{-1}. Molar masses obviously resulting from aggregation increased up to approximately $900 \cdot 10^6$ g·mol^{-1}12 hours after t_0. Even at this time the increase was still steady and exponential with no sign of equilibrium, which may be due to equal rates of aggregation and disintegration of fragments.

By addition of L-cysteine to the diluted stratum corneum centrifugates, the aggregation process was suppressed in a concentration-dependent mode. It was found that L-cysteine reduced the molar masses at the beginning of the experiment (Fig. 1(a)), whereas after 5.5 hours a 10-fold increase of the molar masses was observed comparable to the saline-diluted samples. In samples diluted with 0.1 mol L-cysteine-saline, the molar masses increased from 2 to $20 \cdot 10^6$ g·mol^{-1} over the time period of 5.5 hours.

In double-logarithmic plot (see [38]) rms radii were correlated in a linear mode with molar masses at various times after t_0 over the complete experimental period (Fig. 1(b)). In linear regression using least square to fit a slope of 0.46 was calculated. (rms radius = 0.24 M$^{0.46}$, regression coefficient $r^2 = 0.971$.)

3.2. Transmission electron microscopy

Within the glutaraldehyde-fixed gel (4 hours after centrifugation), we observed numerous membrane-coated lipid droplets varying from 0.1 to 1 μm, embedded within polymorphic clusters formed by cross-linked proteinaceous gel components during fixation (Fig. 2). We detected no fibers in these polymorphic clusters.

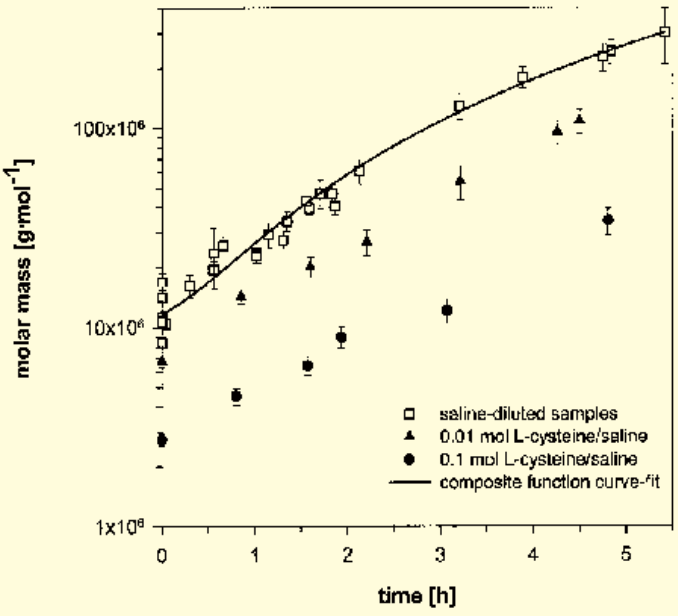

(a)

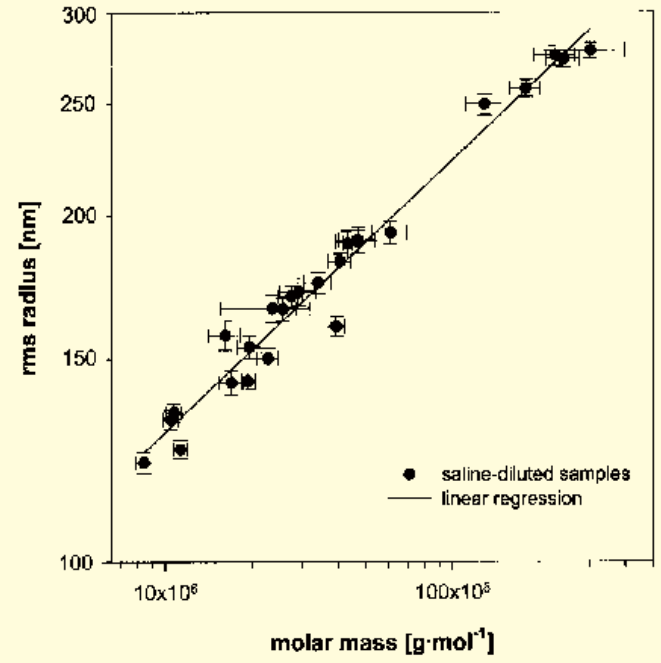

(b)

Fig. 1. (a) The time-dependent increase in the molar mass of fifteen centrifuged and diluted stratum corneum samples (approx. 1 : 500). By addition of L-cysteine, preaggregates disassembled followed by the slow increase of the molar masses during the experiment. (b) The linear correlation of rms radius and the molar mass of various diluted stratum corneum samples (approx. 1 : 500) (double logarithmic plot).

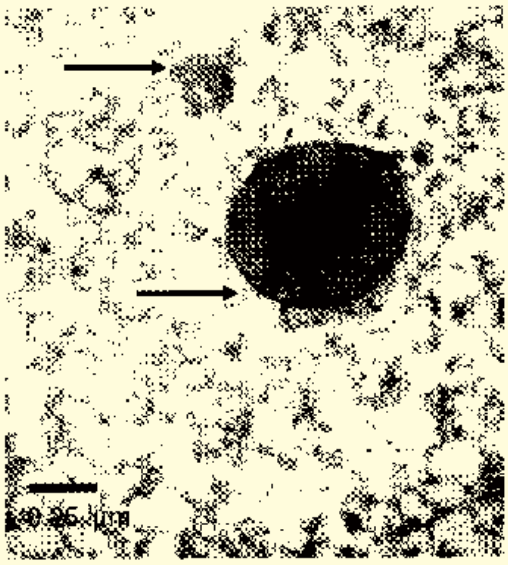

Fig. 2. Within the gel fixed with 2% glutaraldehyde and postfixed with 2% osmium acid, membrane coated (arrows) lipid droplets were embedded within polymorphic clusters of aldehyde-linked proteinaceous gel components. Transmission electron microscopy.

3.3. Rheology

The gel kinetic experiments showed that the undiluted centrifuged stratum corneum transformed from sol to gel (viscoelastic fluid/solid). We standardized handling procedures prior to data collection to ensure that handling time was held constant (5 minutes) and of negligible duration compared to the experimental time. Kinetic data obtained were the same under stress-controlled and deformation-controlled experimental conditions, but the curves of observed gel formation shifted to the left, and cross-over events occurred approx. one hour earlier when using higher speed centrifugation (4000 U/min instead of 3000 U/min). In this study, concentration of undiluted samples varied and the kinetic evolution of the system deferred to a minor extent of about 10 minutes in regard to the cross-over times.

The gel kinetics of undiluted samples (protein concentration approx. 0.062 $g \cdot ml^{-1}$, centrifuged at 3000 U/min) were characterized by initially low undulating values of the storage modulus G' (solid line in Fig. 3) and the loss modulus G'' (dotted line in Fig. 3). After approximately 1.5 hours (t_0, end of centrifugation, 3000 U/min), the cross-over event marked the gel formation ($G' = G'' = 0.063$ Pa, frequency $\omega = 0.35$ rad$\cdot s^{-1}$, stress $\tau = 0.27$ Pa, temperature 20°C). It was remarkable, that both moduli increased strongly in the following 3.5 hours ($G' = 600$–800 Pa, $G'' = 100$–200 Pa), and subsequently G' and G'' further increased until they were fluctuating around 800 to 1000 Pa for the next 12 hours (data not shown). In the late gelling phase (after 3 hours), the capacity to dissipate free energy increased in undiluted sample preparations as indicated by the increase in the loss modulus G''.

The values of G' and G'' normalized to the temperature of 20°C decreased at cross-over events with dilution (Fig. 4). Whereas the decrease of G' was moderate below the dilution of 1 : 10, G' strongly decreased from undiluted samples to dilutions of 1 : 10. Since moduli as a function of concentration are often represented in gel rheology by a power law (see [25]), we fitted slightly smoothed data using the power law equation $f = y_0 - ax^{(b)}$ ($y_0 = -0.01$, $a = 1.50$, $b = 1.12$, regression coefficient $r^2 = 0.9995$).

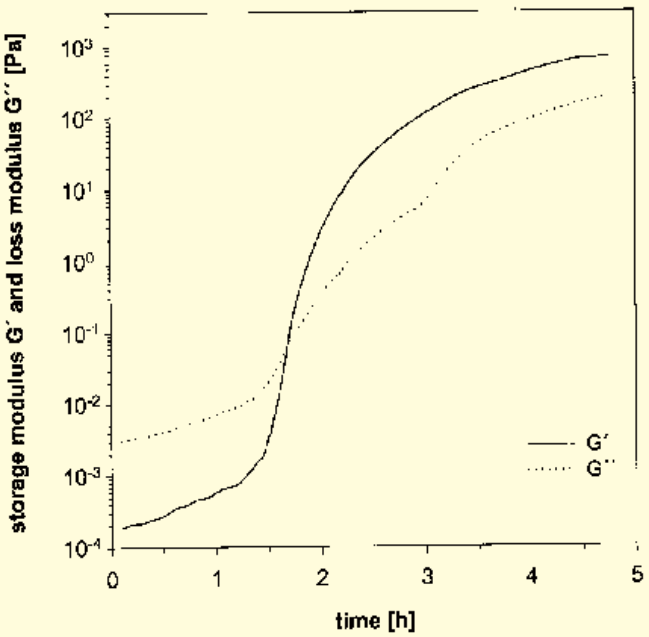

Fig. 3. Stess-controlled gelation kinetics of the undiluted intercorneocytes material (at $\tau = 0.27$ Pa, $\omega = 0.35$ rad·s^{-1}, 20°C, centrifuged at 4000 U/min, protein concentration 0.062 g·ml^{-1}) collected from the corneocytes of *G. melas*. The fluid transformed from sol to gel. Data of G'' were smoothed within the time interval of 3 to 5 hrs.

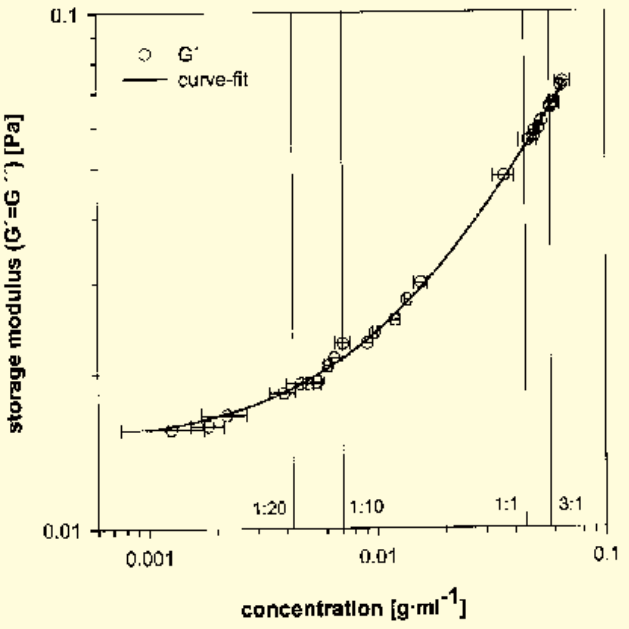

Fig. 4. Concentration dependence of cross-events of diluted and undiluted preparations of the centrifuged stratum corneum of the pilot whale (double logarithmic plot). Values of the storage modulus at cross-over events were fitted to a power law equation.

Mechanical spectra were recorded in alternation at frequencies decreasing and increasing between $\omega = 43.98$ to 0.03 rad·s^{-1} ($\tau = 15$ Pa, $T = 20$°C) loading undiluted samples (results from various sweeps between $\omega = 43.98$ to 0.13 rad·s^{-1} of one sample shown in Fig. 5(a), (b)). No slippage-effect was observed within this range of frequencies. Data were nearly independent of the mode of the sweep but, in general, revealed an increase in G' (approx. 1200–2800 Pa, Fig. 5(a)) and G'' (approx. 10–200 Pa, Fig. 6(b)) with longer delay times from cross-over events. It was evident, that G' and G'' were nearly independent of frequency, whereas G' was one (in older gels) to two (in younger gels) orders of magnitude higher than G''. It is notable, that G'' (in Fig. 5(b)) peaked around $\omega = 0.35$ rad·s^{-1} corresponding to the frequency used during gel formation (as the history of the load applied). This effect was completely reduced in aged gels (delay of 9.5 hours after centrifugation). We always recorded a drop of G'' at approximately $\omega = 20$ to 30 rad·s^{-1}, and observed that during increasing measurement time (at low frequencies), G' and G'' strongly increased at frequencies below $\omega = 0.13$ rad·s^{-1} due to the gel formation proceeding during the measurement. We therefore excluded these values from the mechanical spectrum.

At the frequency $\omega = 0.35$ rad·s^{-1}, under which the gel had formed, stress amplitude sweeps were performed in order to evaluate the strain resistance of the undiluted samples (Fig. 6). Younger gels (5.5 hours after centrifugation, circles in Fig. 6) displayed strain hardening as indicated by the high values of G' increasing between $\gamma = 0.08$–75% combined with shear thinning due to the slightly decrease in G'' in the same range of deformation. After a deformation of $\gamma = 75\%$, the gel collapsed and the values G' and G'' rapidly declined to approx. 1 Pa. In aged gels (9.5 hours after cross-over, squares in Fig. 6), values of G' and G'' were two orders of magnitude higher. In aged gels, strain hardening between $\gamma = 0.2$–1% as obvious from the slight increase of G' was followed by the rheodestructive impact of the load on the structure at approximately $\gamma = 1\%$ (determinating the end of linear viscoelasticity). As observed in younger gels, in aged gels G' and G'' rapidly declined below 2 Pa after a deformation of $\gamma = 75\%$. At this deformation, the stress τ reached approx. 300 Pa in younger gels and approx. 8000 Pa in aged gels.

4. Discussion

4.1. Multi-angle laser light scattering and transmission electron microscopy

According to the multi-angle laser light scattering analysis of highly diluted centrifuged stratum corneum abrasions of the pilot whale skin, the components in the sample formed aggregates. This was predicted from the aggregation observed in semi-diluted samples employing size exclusion chromatography and Native PAGE [7]. In semi-diluted samples [7], high molar mass aggregates between 250–2000 kD and lower molecular weight fractions of about 20 to 30 kD were considered to be involved in gel formation by potentially cross-linking themselves into multiples and aggregates. The high molar masses measured in the study represented weight-average values of a mixture. We found that the molar masses and the rms radii were linearly correlated over the whole experimental period. The double-logarithmic plot of rms radius versus molar mass yields information about the molecular conformation of the samples, similar to the Kuhn–Mark–Houwink plot. In both cases the slope of the function corresponds to the conformation, whereby a slope of 0.33 is indicative for solid spheres, a slope between 0.5 and 0.6 is usually found for linear polymers with random coil conformation, and a slope of 1 for rods [38]. The slope of 0.46 measured hints at molecules slightly more compact than statistical molecules. But it is important to aware that this is true for samples with equal polydispersity only, for the samples of the centrifuged stratum corneum we have to assume different polydispersity (compare [7]).

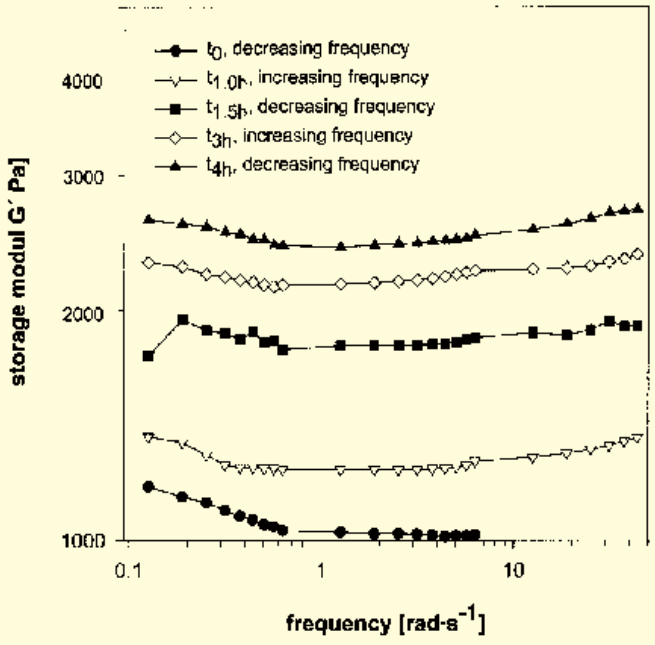

(a)

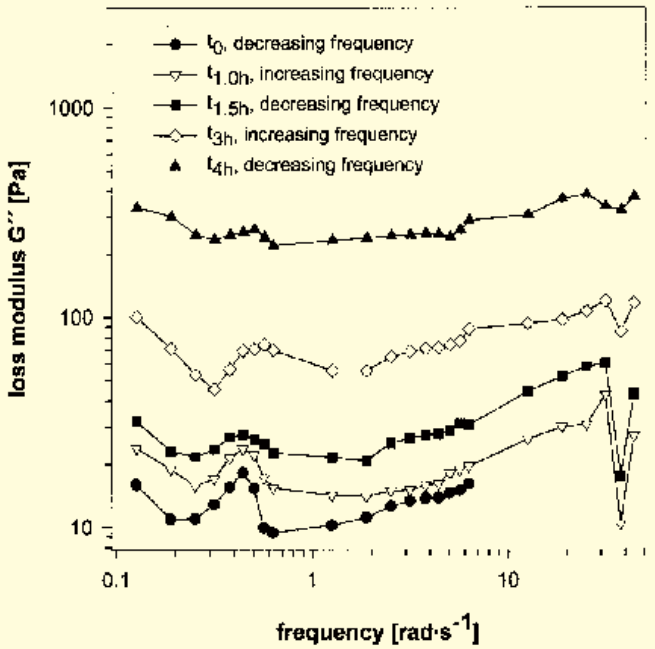

(b)

Fig. 5. (a) Frequency sweeps of alternating decreasing and increasing frequencies $\omega = 42.98$ to 0.13 rad·s^{-1} ($\tau = 15$ Pa, $T = 20$°C). Loads were applied to the same undiluted sample at five different delay times after cross-over points (compare Fig. 3). The storage modulus G' was independent of frequency, but showed a slight increase at lower frequencies due to the continuing gel formation at prolonged measurement time. (b) Frequency dependency of the loss modulus G'' corresponding to the values of G' (Fig. 6(a)). G'' peaked around 0.35 rad·s^{-1} and decreased at 20–30 rad·s^{-1}. G'' was one to two orders of magnitude lower than G' (compare with Fig. 6(a)).

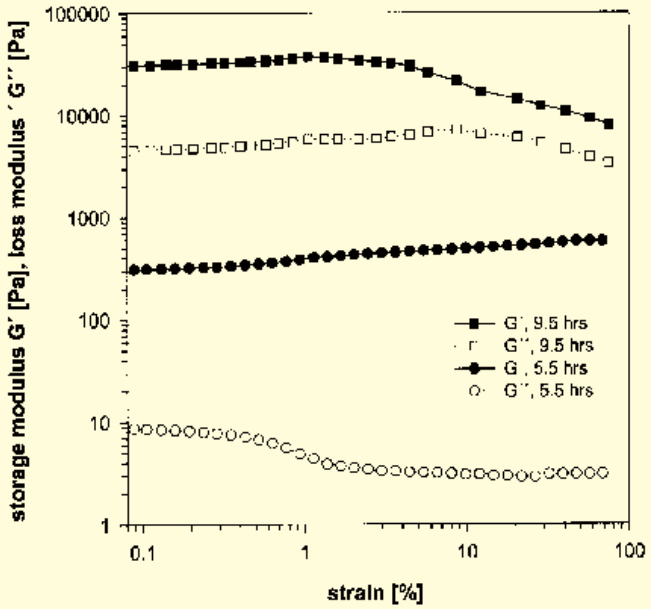

Fig. 6. Strain sweep at increasing deformation γ from $\gamma = 0.08-75\%$ ($\omega = 0.35$ rad·s^{-1}, $T = 20^{\circ}$C) applied to the undiluted gel at two different delay times after centrifugation. The younger gel showed shear thinning and also strain hardening.

With respect to the time-dependent exponential increase of the molar masses, we conclude that in the initial step of the aggregation, nucleation centres are continuously established from smaller molecules as followed by aggregative linkages of such centres to form secondary aggregates. This result was consistent with our previous observation that the biogel forming process had started with the nucleation of smaller elements [7]. The formation of secondary aggregates observed in multi-angle laser light scattering experiments was in aggreement with the gel kinetics (see below), wherein the formation of structuring elastic elements increased during the biogel forming process. Although molar mass and the physical parameters cannot be directly compared, the time-dependent changes and because the formation of the gel and the aggregates was not terminated even after long experiment, both are suggestive for this development of elastic aggregates mentioned above.

The initial L-cysteine-induced reduction of the molar masses was followed by a slow increase of the molar mass. Thus, the assembly of preformed high mass aggregates from smaller fragments was reversed. In contrast to the chaotropic impact on the preaggregates at the beginning of the experiments that was expected to suppress the reconstitution of higher molar masses especially at high concentration of L-cysteine, the reconstitution was not inhibited. Therefore it was questioned, whether the aggregate formation was accompanied by additional reactions influenced by L-cysteine, in particular, covalent cross-linking reactions corresponding to the mechanical properties obtained (see below). L-cysteine exhibits a mild oxidizing potential to free thiol groups suggesting that L-cysteine unbalanced covalently cross-linking reactions and phase separation during the aggregate formation of the centrifuged stratum corneum. It also increased the solubility of thiol-containing polypeptides cross-linked with this aminoacid, and thus reduced the molar masses of aggregating components. Further investigations are planned, focussing on the reconstitution of aggregates and the formation of disulfide bridges, which supposedly belong to the main primary processes of gel formation. With respect to the rheological properties of the gel displaying features of covalently cross-linked gels (see below), we suggest that keratin

polypeptides, which are the major disulfide-containing components in the epidermis [33], are involved in the gel forming process.

Thin sections of glutaraldehyde-fixed *in vitro* gels revealed the presence of numerous membrane-coated lipid droplets, embedded within polymorphic clusters of aldehyde-linked proteinaceous gel components. We assume that the membrane-coated inclusions are lipids, which are usually globular and not denatured by aldehydes. In addition, we suggest that the lipid inclusions are no artifacts formed during the experiment, but are native components in the stratum corneum of the pilot whale, since such droplets were also present on electron micrographs of freeze-etched intact non-fixed and osmium-fixed epidermis [5,29].

With respect to the membranes coating the lipids, it seems reasonable to conclude that the membranes are amphiphilic, since they connect the hydrophobic lipids and the hydrophilic gel. Assuming that the biopolymeric gel is a typical hydrogel enclosing water within the three-dimensional network of macromolecules, the presence of the lipids demonstrated is an evidence of a three-phase-system. In this system the actual high energy of forced load overshoots can be transferred to both the viscous lipids and to the viscoelastic network. In dolphins, a three-phase-system seems to be especially suited to the anticipated high load, especially during jumping. As described in a previous study by Baum et al. [5], the skin surface (and the intercorneocyte space, unpublished results) exhibits alternating hydrophilic and hydrophobic sectors located within a relief of desmosomal nanoridges, which are considered as the most prominent skin surface characteristics. These sectors should originate from the above-described subcellular separation into a hydrophilic and a hydrophobic phase.

In the first and only rheological experiments until now investigating the highly diluted delphinid stratum corneum suspended in seawater using the Ostwald viscometer [31], the viscosities of the suspension were marginally higher than that of seawater. This result contrasted to the preliminary assumption of the authors, who expected polymers within the suspension efficient in minimizing drag to increase the elongational viscosity of seawater [23]. According to the physical properties of the intercorneocyte fluid observed in our study, the viscosities measured in the above-reported publication [31] are in agreement with the high self-aggregating performance of the stratum corneum components contributing to the formation of aggregated particles rather than hydrated solubilized macromolecules. Solubilized macromolecules reducing drag, such as glycoconjugates, are known, for example, from mucoid secretions of fish [22].

4.2. *Rheology*

Because the corneocytes of dolphins are surrounded by a macromolecular coating [18], we have demonstrated here that a fluid containing the coating material collected from the intercorneocyte space of the epidermis of the pilot whale transformed from sol to gel, forming a biogel. Since it is evident that a gel fills the space between the uppermost five to six layers of the stratum corneum (unpublished), which are not in contact with seawater with potential to dilute the intercorneocyte material, we argue that the gel formation *in vivo* corresponds to our results on the undiluted sample *in vitro*.

The gel formation terminates in the assembly of a viscoelastic solid. Identical kinetic values were obtained under both stress-controlled and deformation-controlled experimental conditions, indicating independency of the gel kinetics from the kind of load applied. In contrast we found that in the mechanical spectra recorded the loss modulus of younger gels peaked around the frequency applied during gel kinetic experiments. This damping effect, potentially based on resonance, was completely reduced in aged gels. Further investigations are planned to analyze such damping effect in the dependency of various loads. We standardized handling procedures prior to data collection and ensured that handling

time was held constant and negligibly low compared to the experimental time. Handling procedure included centrifugation at constant speed and time. Before measurements, the samples were pooled from the fractions centrifuged, alternatively diluted, loaded and covered by the vapor trap within 5 minutes. The curves of gel formation shifted to the left, and cross-over events occurred approx. one hour earlier when using higher speed centrifugation (4000 U/min instead of 3000 U/min). Traces of gel kinetics were reproducible when using aliquots of the same centrifugate. Because the concentration of undiluted samples varied slightly due to the varying water up-take during centrifugation, the differences of gel kinetics between different undiluted samples displaying the same qualities and segmented curves indicated that gel kinetics were highly dependent of concentration. It was found, that cross-over systematically occurred earlier in less concentrated samples and values of the moduli were lower after gel formation. We sorted storage moduli (at $G' = G''$) of various undiluted and diluted samples by sample concentration assayed by the Bradford glycoprotein assay or extrapolated concentration from the signals of the refractive index detector (compare [7]). The correlation established in this study indicates that the Bradford assay and the signals of the refractive index detectors can be used to evaluate the concentration of the samples, whereby the extrapolation was preferred. Due to the fact that the conjugation of the stain may potentially be restricted to the external surfaces of the aggregates, the Bradford assay can be misleading in measuring the concentration of particularly highly concentrated glycoprotein-rich samples. However, in order to compare the gel kinetics of different delphinid species, we think that it would be better to define the sample concentration based on specific gel forming components in addition to the content of glycoproteins.

The mechanical spectra of the undiluted polymerized gel showed that G' and G'' were independent of frequency over a range of more than two decades, and, in addition, that the plateau region of G' was more than one order of magnitude higher than G''. These properties of the gel match with covalently cross-linked structural gels [17]. Since the shear thinning effects observed during strain sweeps were reduced in aged gels, shear thinning is indicative of both entangling and cross-linked aggregates, whereby the gel formation of undiluted samples is clearly dominated by the perpetual cross-linking of the aggregates. It is suggested that reactions are based on affinity of non-covalent cross-linked aggregates (cooperative effects) as well on covalent cross-linking reactions (accumulative effects). Further experiments are planned to investigate specific interactions of molecules of the stratum corneum in connection with segmented analysis of the gel kinetic data using more-event gamma distribution functions. The results of this analysis are in aggreement with the conclusion from the strain sweep experiments, indicating the involvement of non-covalent and covalent aggregation processes during the gel formation of the centrifuged stratum corneum. Considering the impact on the aggregation process by L-cysteine, we suggest that free thiol groups are involved in the cross-linking reactions. Comparable to the network properties of the heteropolymeric keratin filament aggregates [24], we detected that the centrifuged stratum corneum of the pilot whale investigated in this study displayed strain hardening followed by a rapid yield of the strain resistance. Unlike the preparations of keratin heteropolymers [24], no filament aggregates were present in the gel tested. Therefore the shear thinning effects observed may be based on the presence of smaller elements than filament aggregates, manifesting stiffer viscoelastic gels combined with higher internal motility.

Since in the post-gelling phase both moduli increased, we argue that the energy of the load was stored elastically and dissipated during the experiment. So the energy may be transferred from the above-mentioned viscoelastic-proteinaceous compartment into the viscous-lipid compartment.

Considering the profile of the mechanical spectra, the gel displayed high elastic performance. The stress damped at low frequencies ω (ω below 0.62 rad·s^{-1}) as indicated by the slight increase of the

loss modulus G'' concomitant with the slight decrease of the storable free energy (not shown), and could be caused the less effective activation of the viscoelastic network. The energy transferred into the lipid droplets, however, can dissipate the energy of the load. These results showed that the gel was shear resistant under stress conditions for more than several minutes. Since swimming, jumping and long-term distance migration of dolphins, in particular, may induce high values of stress to the skin surface, the measured gel characteristics indicating high stress resistance and structural integrity of the stratum corneum, corroborate the important biological functions of this skin product.

The high elastic performance and the inclusion of lipids clearly contrasts with the biochemical and rheological properties of polysaccharide-based entangled gels originating from colloids, gel-particles or biofilms of microfouling organisms [9,15,27,30,34,35]. Absorbed by the charged and hydrophobic surfaces of organisms or ship hulls, such adhesive organic matter forms a conditioning organic layer. Microfouling organisms attaching to and growing on this layer, initiate the formation of a mucilagineous, mainly polysaccharide-based, biofilm [10,16,34,37]. Compared to the high elastic performance of the centrifuged gel of the delphinid stratum corneum, the elastic storage modulus of algal exudates and bacterial biofilms are 1–2 orders of magnitude lower (20–40 Pa) [28,30,34,35]. In addition, lower values of the wall stress τ reported in biofilms indicate a lower shear resistance of the biofilms than that of the polymerized gel medium collected from the stratum corneum of the pilot whale. Since during jumping of the dolphin shear stress is induced by the contact with an air-liquid interface or high water flow, we argue from our experiments that the gel filling the intercorneocyte space smoothing the skin surface [8] can withstand higher shear stress regimes than the mucoid contaminations. Therefore, contaminations are detached from the skin surface under shear stress regimes, which do not affect the structural integrity or the position of the gel within the intercorneocyte space or the upper side of the stratum corneum.

We know from one of our previous studies [7], that the above-reported gel medium contains a variety of hydrolytic enzymes. Considering the higher shear resistance of this gel compared with the biofilms, the gel properties can, additionally, guarantee the retention of active hydrolytic enzymes in the superficial layers of the skin during the jumping. Hydrolytic enzymes digesting the desmosomal junctions in order to initiate the desquamation process probably remove contaminations as large as the desquamating corneal cells. Moreover, enzymes may hydrolyze adhesive mucilagineous glycoconjugates used by biofoulers for attachment. Therefore, the retention of enzymes to some extent broadens the self-cleaning abilities of the dolphin integument.

With respect to the relief of pores derived from the desmosomal nanoridges filled by the gel [8], the latter obscures the surfaces of the corneocytes, forming an even plane surface with lateral irregularities less than 30 nm. Such a smooth surface exhibits no particular microniches, in which biofouling organisms are protected against shear stress or desorptive air-bubbles during jumping.

Comparing all these aspects, we can conclude that gel-forming abilities and properties of this gel (high shear resistance, high stress damping, alternating chemical surface activity, hydrolytic activity and skin smoothing) described in this study are indispensable for the self-cleaning abilities of the dolphin skin.

Acknowledgements

The authors thank Dr. D. Bloch and Mr. E. Stefansson, Museum of Natural History, Faroe Islands, Mrs. J. Zachariasen, Mrs. M. Mortensen and Dr. H.-P. Joensen, University of the Faroe Islands, for their help in specimen collection for legal harvest. We are grateful to Dr. C. Johann and Mr. J. Wellensiek, Wyatt Technology Germany, for their technical assistance in MALLS measurements. The authors also thank

Dr. R. Crawford, Alfred Wegener Institute Foundation for Polar and Marine Research and the reviewers for discussing the manuscript and many valuable suggestions. This study was supported by a grant of the Deutsche Forschungsgemeinschaft DFG (ME 1755 1-1/1-2).

References

[1] S. Abarzua and S. Jakubowski, Biotechnological investigation for prevention of biofouling. I. Biological and biochemical principles for the prevention of biofouling, *Mar. Ecol. Progr. Ser.* **123** (1995), 301–312.
[2] J.B. Alexander and G.A. Ingram, Non-cellular non-specific defence mechanisms of fish, *Annu. Rev. Fish Dis.* **2** (1992), 249–279.
[3] L.I. Aluwihare, D.J. Repeta and R.F. Chen, A major biopolymeric component to dissolved organic carbon in surface sea water, *Nature* **387** (1997), 166–169.
[4] L.I. Aluwihare and D.J. Repeta, A comparison of the chemical characteristics of oceanic DOM and extracellular DOM produced by marine algae, *Mar. Ecol. Prog. Ser.* **186** (1999), 105–117.
[5] C. Baum, R. Stelzer, W. Meyer, D. Siebers and L.-G. Fleischer, A cryo-scanning electron microscopic study of the skin surface of the pilot whale *Globicephala melas*, *Aquatic Mammals* **26** (2000), 7–16.
[6] C. Baum, L.-G. Fleischer, W. Meyer, D. Siebers and R. Stelzer, Gelations kinetics of a gel collected from the corneocytes of the pilot whale (*Globicephala melas*), *Zoology* **104**(Suppl. 4) (2001), 53.
[7] C. Baum, W. Meyer, D. Roessner, L.-G. Fleischer and D. Siebers, A zymogel enhances the self-cleaning abilities of the pilot whale (*Globicephala melas*), *Comp. Biochem. Physiol. A* **130** (2001), 835–847.
[8] C. Baum, W. Meyer, R. Stelzer, L.-G. Fleischer and D. Siebers, The average nanorough skin surface of the pilot whale (*Globicephala melas, Delphinidae*): considerations on the self-cleaning abilities based on nanoroughness, *Mar. Biol.* (2002), DOI 10.1007/300227-001-0710-8.
[9] K. Becker, Detachment studies on micofouling in natural biofilms on substrata with different surface tensions. *Int. Biodeter. Biodegrad.* **41** (1998), 93–100.
[10] T.J. Beveridge, S.A. Makin, J.L. Kadurugamuva and Z. Li, Interactions between biofilm and the environment. *FEMS Microbiol. Rev.* **20** (1997), 291–303.
[11] D. Bloch, G. Desportes, R. Mouritsen, S. Skaaning and E. Stefansson, An introduction to studies of ecology and status of the long-finned pilot whale (*Globicephala melas*) of the Faroe Islands, 1986–1988, *Rep. Int. Whal. Comm.* (Special issue) 14 (1993), 1–32.
[12] R. Bos, H.C. van der Mei, J. Gold and H.J. Busscher, Retention of bacteria on substratum surface with micro-patterned hydrophobicity, *FEMS Microbiol. Let.* **189** (2000), 311–315.
[13] W.R. Brown, J.R. Geraci, B.D. Hicks, D.J. St.Aubin and J.P. Schroeder, Epidermal cell proliferation in the bottlenose dolphin *Tursiops truncatus*, *Can. J. Zool.* **61** (1983), 1587–1590.
[14] A.S. Clare, Marine natural product antifouling: status and potential, *Biofouling* **9** (1996), 211–229.
[15] W.-C. Chin, M.V. Orellana and P. Verdugo, Spontaneous assembly of marine dissolved organic matter into polymer gels, *Nature* **391** (1998), 568–572.
[16] K.E. Cooksey and B. Wigglesworth-Cooksey, Adhesion of bacteria and diatoms to surfaces in the sea: a review, *Aquat. Microb. Ecol.* **9** (1995), 87–96.
[17] J.D. Ferry, *Viscoelastic Properties of Polymers*, John Wiley, New York, 1980.
[18] J.R. Geraci, D.J. St. Aubin and B. Hicks, The epidermis of odontocetes: a view from within. in: *Research on Dolphins*, Vol. 1, M.M. Bryden and R. Harrrison, eds, Clarendon Press, Oxford, 1986, pp. 3–21.
[19] H. Gucinski, R.E. Baier, A.E. Meyer, M.S. Fornalik and R.W. King, Surface microlayer properties affecting drag phenomena in seawater, in: *Proceedings of the 6th Marine Corrosion Congress*, Athens, Greece, 1984. pp. 1–24.
[20] H. Gucinski, Correlation of biophysical surface characteristics with hydrodynamic properties of adhesive biofilms, State University of New York at Buffalo, PhD dissertation, 1986.
[21] D.B. Hicks, D.J. St.Aubin, J.R. Geraci, W.R. Brown, Epidermal growth in the bottlenose dolphin, *Tursiops truncatus*, *J. Invest. Dermatol.* **85** (1985), 60–63.
[22] J.W. Hoyt, Hydrodynamic drag reduction due to fish slimes, in: *Swimming and Flying in Nature*, Vol. 2, Y. Theodore, C.J. Brokaw and C. Brennen, eds, Plenum Press, New York, 1975, pp. 653–672.
[23] J. Klein, Smart polymer solution, *Nature* **405** (2000), 745–747.
[24] L. Ma, Xu Jingyuan, P.A. Coulombe and D. Wirtz, Keratin filament suspensions show unique micromechanical properties, *J. Biol. Chem.* **274** (1999), 19 145–19 151.
[25] A.G.J. Mac Farlane, *Engineering Systems Analysis*, G.G. Harrap & Co, London, 1967.
[26] K. te Nijenhuis, Thermoreversible networks – viscoelastic properties and structure of gels, *Adv. Polym. Sci.* **130** (1997), 1–252.

[27] U. Passow, Formation of transparent exopolymer particles, TEP, from dissolved precursor material, *Mar. Ecol. Progr. Ser.* **192** (2000), 1–11.
[28] C. Picioreanu, M.C. van Loosdrecht and J.J. Heijnen, Two-dimensional model of biofilm detachment caused by internal stress from liquid flow, *Biotech. Bioeng.* **72** (2000), 207–218.
[29] C.J. Pfeiffer and F.M. Jones, Epidermal lipid in serveral cetacean species: ultrastructural observation, *Anat. Embryol.* **188** (1993), 209–218.
[30] J. Ramus and B.E. Kenney, Shear degradation as a probe of microalgal exopolymer structure and rheological properties, *Biotechnol. Bioeng.* **34** (1989), 1203–1208.
[31] W. Sokolov, I. Bulina and V. Rodinov, Interaction of dolphin epidermis with flow boundary layer, *Nature* **222** (1969), 267–268.
[32] D.J. St. Aubin, T.G. Smith and J.R. Geraci, Seasonal epidermal molt in beluga whales, *Delphinapterus leucas*, *Can. J. Zool.* **68** (1990), 359–367.
[33] P.M. Steinert, Epidermal keratin: filament and matrix, in: *Stratum Corneum*, R. Marks and G. Plewig, eds, Springer, Berlin, 1983, pp. 25–38.
[34] P. Stoodley, Z. Lewandowski, J.D. Boyle and H.M. Lappin-Scott, Structural deformation of bacterial biofilms caused by short-term fluctuations in fluid shear: An in situ investigation of biofilm rheology, *Biotech. Bioeng.* **65** (1999), 83–92.
[35] I.W. Sutherland, Structure–function relationship in microbial exopolysaccharides, *Biotechnol. Adv.* **12** (1994), 393–448.
[36] T.R. Tosteson, The regulation and specificity of marine microbial surface interactions, in: *Biotechnology of Marine Polysaccharides*, Session III, R.P. Colwell, E.R. Parisier and A.J. Simskey, eds, Hemisphere Publishing Corporation, Washington, 1984, pp. 77–114.
[37] M. Wahl, Marine epibiosis. I. Fouling and antifouling: some basic aspects, *Mar. Ecol. Prog. Ser.* **58** (1989), 175–189.
[38] P.J. Wyatt, Lightscattering and absolute characterisation of macromolecules, *Analyt. Chim. Acta* **272** (1993), 1–40.